Published OnlineFirst February 1, 2013; DOI: 10.1158/0008-5472.CAN-12-1472

Cancer Research

Involvement of Lyn and the Atypical Kinase SgK269/PEAK1 in a Basal Breast Cancer Signaling Pathway

David R. Croucher, Falko Hochgräfe, Luxi Zhang, et al.

Cancer Res 2013;73:1969-1980. Published OnlineFirst February 1, 2013.

Published OnlineFirst February 1, 2013; DOI: 10.1158/0008-5472.CAN-12-1472

Involvement of Lyn and the Atypical Kinase SgK269/PEAK1 in a Basal Breast Cancer Signaling Pathway

David R. Croucher, Falko Hochgräfe, Luxi Zhang, Ling Liu, Ruth J. Lyons, Danny Rickwood, Carole M. Tactacan, Brigid C. Browne, Naveid Ali, Howard Chan, Robert Shearer, David Gallego-Ortega, Darren N. Saunders, Alexander Swarbrick, and Roger J. Daly

Abstract

Basal breast cancer cells feature high expression of the Src family kinase Lyn that has been implicated in the pathogenicity of this disease. In this study, we identified novel Lyn kinase substrates, the most prominent of which was the atypical kinase SgK269 (PEAK1). In breast cancer cells, SgK269 expression associated with the basal phenotype. In primary breast tumors, SgK269 overexpression was detected in a subset of basal, HER2-positive, and luminal cancers. In immortalized MCF-10A mammary epithelial cells, SgK269 promoted transition to a mesenchymal phenotype and increased cell motility and invasion. Growth of MCF-10A acini in three-dimensional (3D) culture was enhanced upon SgK269 overexpression, which induced an abnormal, multilobular acinar morphology and promoted extracellular signal–regulated kinase (Erk) and Stat3 activation. SgK269 Y635F, mutated at a major Lyn phosphorylation site, did not enhance acinar size or cellular invasion. We show that Y635 represents a Grb2-binding site that promotes both Stat3 and Erk activation in 3D culture. RNA interference–mediated attenuation of SgK269 in basal breast cancer cells promoted acquisition of epithelial characteristics and decreased anchorage-independent growth. Together, our results define a novel signaling pathway in basal breast cancer involving Lyn and SgK269 that offers clinical opportunities for therapeutic intervention. *Cancer Res; 73(6); 1969–80. ©2012 AACR.*

Introduction

Basal breast cancers usually exhibit a "triple-negative" receptor phenotype and are therefore resistant to endocrine or trastuzumab therapy (1). The identification of novel therapeutic targets for this clinically aggressive subgroup represents a high priority. We recently used phosphoproteomic profiling to identify a signaling network associated with basal breast cancer cells that is governed by Src family kinases (SFK; ref. 2). The SFK Lyn was a prominent member of this network, which also contained the atypical kinase Sugen Kinase 269 (SgK269) also termed PEAK1 (3).

SgK269, along with SgK223, comprises the new kinase family 3 (NKF3) of protein kinases. Although both proteins exhibit substitutions within the critical DFG, a triplet of the kinase domain activation loop, leading to their initial classification as pseudokinases (4, 5), the Klemke group has reported that SgK269 possesses weak tyrosine kinase activity (3). In addition, SgK269 is tyrosine-phosphorylated downstream of several tyrosine kinases (6–11). SgK269 localizes to the actin cytoskeleton and focal adhesions and associates with p130Cas and Crk, indicating that it may regulate cytoskeletal organization (3). SgK269 expression is induced by active Ras in a Src-dependent manner, and in preclinical models of pancreatic cancer, promotes tumor growth, metastasis, and resistance to specific therapies (12).

In this study, we refine the network downstream of Lyn in basal breast cancer cells, identifying SgK269 as a target of Lyn phosphorylation. We also characterize the functional role of SgK269 in mammary epithelial and basal breast cancer cells and determine that Lyn regulates a novel scaffolding function of this kinase.

Materials and Methods

Plasmids

A cDNA encoding N-terminal HA-tagged and C-terminal His/Myc-tagged SgK269 was generated by nested PCR from a human SgK269 cDNA in pCMV6 (Origene) and cloned into the *Sac*II and *Bam*HI restriction sites of the pRetroX-IRES-DsRed Express vector (Clontech). The pSIREN-RetroQ-ZsGreen (Clontech) constructs containing short hairpin RNA (shRNA) targeting SgK269 and GFP (negative control) were constructed by the ligation of synthesized oligonucleotides into the *Bam*HI and *Eco*RI sites of pSIREN. The negative control sequence targeting GFP has been

Authors' Affiliation: Cancer Research Program, The Kinghorn Cancer Centre, Garvan Institute of Medical Research, Sydney, New South Wales, Australia

Note: Supplementary data for this article are available at Cancer Research Online (http://cancerres.aacrjournals.org/).

Current address for D.R. Croucher: Systems Biology Ireland, University College Dublin, Belfield, Dublin, Ireland; and current address for F. Hochgräfe: Junior Research Group Pathoproteomics, Competence Center Functional Genomics, University of Greifswald, Greifswald, Germany.

Corresponding Author: Roger J. Daly, The Kinghorn Cancer Centre, Garvan Institute of Medical Research, 370 Victoria Street, Darlinghurst, Sydney, NSW 2010, Australia. Phone: 61-2-9355-5825; Fax: 61-2-9355-5870; E-mail: r.daly@garvan.org.au

doi: 10.1158/0008-5472.CAN-12-1472

Published OnlineFirst February 1, 2013; DOI: 10.1158/0008-5472.CAN-12-1472

previously described (13). The pLKO.1 (Thermo Fisher) constructs containing shRNA targeting SgK269 and a nontargeting control were generated by the ligation of synthesized oligonucleotides into the *Age*I and *Eco*RI sites of pLKO.1. Oligonucleotide sequences can be provided upon request.

Antibodies and reagents

All antibodies were from Cell Signaling Technology, except: PY20 (Abcam); SgK269 and Tubulin (Santa Cruz Biotechnology); β-actin (Sigma); Shc, Grb2, and E-cadherin (BD Biosciences); HA (Roche); and glyceraldehyde-3-phosphate dehydrogenase (GAPDH; Ambion). The affinity-purified rabbit antibody selective for SgK269 pY635 was generated by Cambridge Research Biochemicals Ltd by standard procedures.

Tissue culture and generation of stable cell lines

MCF-10A cells stably expressing the murine ecotropic receptor were maintained as previously described (14). All cancer cell lines were obtained from the American Type Culture Collection, except for MDA-MB-231 and T-47D (EG&G Mason Research Institute, Worchester, MA) and MCF-7 (Michigan Cancer Foundation, Rochester, MI). Cell lines were authenticated by short tandem repeat polymorphism, single-nucleotide polymorphism, and fingerprint analyses, passaged for less than 6 months, and cultured as previously described (15). The packaging cell line PlatE was used for retrovirus production, and MCF-10A and breast cancer cells were infected with retrovirus as previously described (13). Stable knockdown of SgK269 expression in MDA-MB-231 cells was achieved by lentiviral-mediated transduction of the corresponding pLKO.1 construct, packaged with VSVG pseudotype in HEK-293 cells, followed by puromycin (0.7 μg/mL) selection. Cell proliferation assays were conducted using MTS reagent (13). Live cell microscopy, tracking analysis, and invasion assays were as previously described (2, 16).

siRNA treatment

Lyn- and Src-selective siRNAs were obtained from Qiagen and Applied Biosystems, respectively. Sequences can be provided upon request. Negative control siRNA was ON-TARGET *plus* nontargeting pool (Dharmacon). siRNA was applied to cells as previously described (13).

SILAC labeling and phosphoproteomic analysis

BT-549 and MDA-MB-231 cells were subject to "light" (Arg 0, Lys 0) or "heavy" (Arg 10, Lys 8) SILAC labeling by standard procedures (17). Ten 80% confluent 15-cm dishes were used per transfection condition. In one experiment, the control and Lyn siRNA–transfected cells were labeled with "light" and "heavy" isotopes, respectively. A replicate experiment was then undertaken with the labels switched. Phosphopeptide enrichment using P-Tyr-100 and PY20 antibodies and mass spectrometry analysis was undertaken essentially as previously described (2, 18). Changes in protein abundance between light and heavy labeled cell populations were determined by tryptic in-gel digestion of SDS-PAGE–separated protein mixtures following standard procedures. Mass spectra were processed with version 1.1.1.14 of the MaxQuant software package (http://www.maxquant.org/) using default settings. Phosphosite identifications were filtered for greater than 0.75 localization probability. To select an appropriate cutoff for selection of Lyn targets, we plotted the frequency distribution of the SILAC phosphosite fold changes and divided the data into 3 terciles with different percentage cutoffs (19). A fold change of 1.2-fold was selected as this defined the 75% to 100% tercile.

Cell lysis, immunoprecipitation, and pull-downs

Cell lysates for immunoblotting and immunoprecipitation were prepared using lysis and radioimmunoprecipitation (RIPA) buffers, respectively (14). Fusion protein pull-downs and peptide competition assays were conducted as previously described (20, 21). The latter used a final concentration of 50 μmol/L peptide.

Quantitative PCR analysis

The AnalytikJena innuPREP RNA Mini Kit was used to extract mRNA. Reverse transcription was conducted with the Reverse Transcription System (Promega). Quantitative reverse-transcription PCR (qRT-PCR) was carried out on an Applied Biosystems ABI 7900 qPCR machine (Absolute Quantification setting) using TaqMan Gene Expression Assays (Applied Biosystems). Standard curves were constructed for each TaqMan probe. and data were analyzed through the $2^{-\Delta\Delta Ct}$ method, corrected for the efficiency of each TaqMan probe and normalized to the *GAPDH* housekeeping gene. The RT^2 Profiler PCR Array for Human EMT (Qiagen) was used for gene expression profiling.

Three-dimensional growth analysis

This was conducted in Matrigel (BD Biosciences; ref. 14). Photographs of acini were taken using a Leica DFC280 camera with Leica Firecam software (Version 1.9). Acinar diameter was measured using ImageJ Software (Version 1.37).

Fluorescence microscopy

This was conducted using a Zeiss Axiovert 200M inverted fluorescence microscope. Digital images were processed using Axiovision software (Version 4.7). Cell preparation and staining were conducted as previously described (22).

Anchorage-independent growth assays

These were undertaken essentially as previously described (2). Resulting colonies were fixed and stained using Diff-Quick (Lab Aids) and photographs taken using a Leica DFC280 camera with Leica Firecam software (Version 1.9). Colonies larger than 30 μm were quantified by visual inspection.

Human breast cancer specimens

These were provided by the Victorian Cancer Biobank, which is supported by the Victorian Government. The project was approved by St Vincent's Hospital Sydney Human Research Ethics Committee (approval number HREC 08/145). All breast cancer samples were grade III carcinoma and classified by immunohistochemistry as luminal (ER+PR+HER2−), HER2-positive (ER−, PR−, HER2+), and basal (ER−, PR−, HER2−).

Published OnlineFirst February 1, 2013; DOI: 10.1158/0008-5472.CAN-12-1472

Results

Identification of Lyn-regulated tyrosine phosphorylation events in basal breast cancer cells

Previously, we determined that basal breast cancer cells are characterized by a prominent SFK signaling network that features high expression of the SFK Lyn (2). To characterize the role of Lyn, we undertook quantitative phosphoproteomic profiling of BT549 and MDA-MB-231 cells following siRNA-mediated Lyn knockdown (Fig. 1A–C). This identified 7 Lyn targets that were common to both cell lines (Fig. 1C; Supplementary Fig. S1). Three were present in our previously identified phosphorylation signature (Supplementary Fig. S2; ref. 2), specifically Talin-1 (TLN1), α/β-Enolase (ENOA/B), and SgK269, whereas Annexin A2 (ANXA2) did not appear in the signature but is a known interaction partner and phosphorylation target of Lyn (23). A decrease in phosphorylation of the network component BCAR3 was only detected in MDA-MB-231 cells. Other proteins identified as Lyn substrates in MDA-MB-231 and/or BT549 cells were not present in the previously identified signature, indicating that they do not exhibit differential phosphorylation between luminal and basal breast cancer cells.

In parallel, we used SILAC to profile protein expression changes following Lyn knockdown. For many putative Lyn substrates, including ANXA2, ENOA/B, and TLN1, this revealed that Lyn knockdown results in reduced relative tyrosine phosphorylation of specific sites, rather than decreased protein expression (Supplementary Fig. S1). Because SgK269 could not

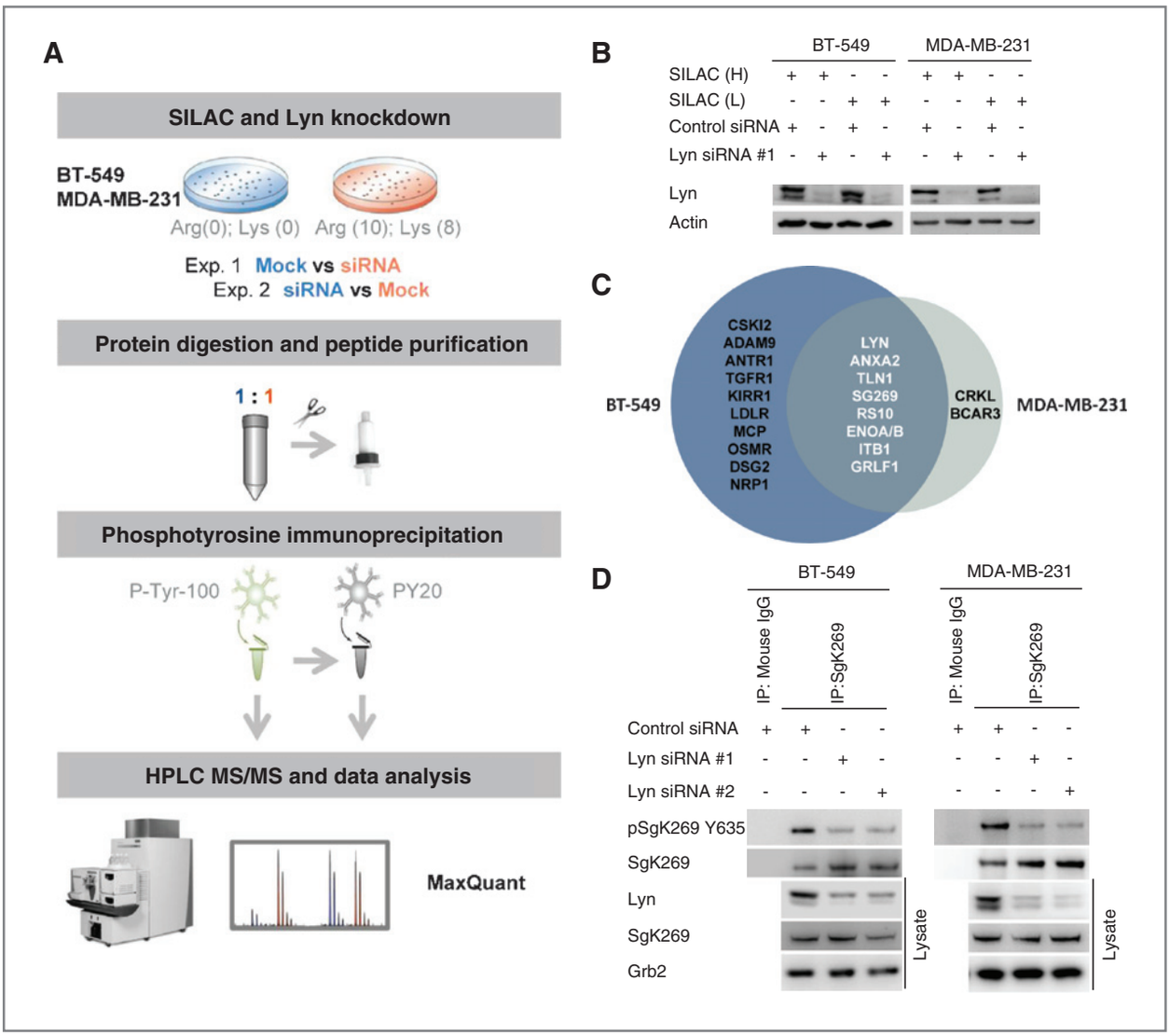

Figure 1. Phosphoproteomic analysis of basal breast cancer cell lines following Lyn knockdown. A, phosphoproteomic profiling workflow. B, validation of Lyn knockdown by Western blotting. C, Venn diagram displaying proteins identified as Lyn substrates in BT-549 and MDA-MB-231 cells. D, biochemical confirmation of Lyn-dependent phosphorylation of SgK269 on Y635. SgK269 immunoprecipitates were Western blotted using a pY635 phosphospecific or total SgK269 antibody. Cell lysates were blotted as indicated. Grb2 served as a loading control.

Published OnlineFirst February 1, 2013; DOI: 10.1158/0008-5472.CAN-12-1472

be detected by mass spectrometric (MS) analysis of total protein lysates, we generated a phosphospecific antibody against one of the Lyn-regulated phosphosites identified, Y635 (Supplementary Fig. S3A). Western blotting of SgK269 immunoprecipitates using this antibody confirmed that relative Y635 phosphorylation is markedly reduced following Lyn knockdown (Fig. 1D). Of note, this decrease was not apparent if the immunoprecipitates were blotted with an anti-phosphotyrosine antibody, indicating that Y635 and the other Lyn-regulated phosphosite Y616 make a relatively small contribution to overall tyrosine phosphorylation of SgK269 (Supplementary Fig. S3B). Overall, these data indicate that Lyn phosphorylates only a small fraction of the previously identified network (Supplementary Fig. S2). This finding was substantiated by blotting of cell lysates with anti-phosphotyrosine and phosphospecific antibodies, which did not reveal major changes in overall tyrosine phosphorylation or in site-specific phosphorylation of the known SFK substrates FAK and BCAR1/Cas following Lyn knockdown (Supplementary Fig. S4).

To further interrogate Lyn function in basal breast cancer, we chose to focus on SgK269, given its recently reported association with several human malignancies (3, 12).

SgK269 expression in breast cancer cell lines and primary breast cancers

Western blotting across breast cancer cell lines revealed that expression of SgK269 is characteristic of the basal phenotype, as observed for Lyn (Fig. 2A; ref. 2). However, this pattern of expression is not reflected in the relative mRNA levels (Fig. 2B), indicating that elevated SgK269 expression in basal breast cancer cell lines must be mediated via a posttranscriptional or posttranslational mechanism. Because the commercial SgK269 antibody is not suitable for immunohistochemistry, we characterized the expression pattern of SgK269 in different subtypes of primary breast cancer by Western blot analysis (Fig. 2C). SgK269 was detected in most of the luminal, HER2, and basal breast cancers analyzed, and for each cancer subtype, a subset of the specimens (20%–40%) exhibited marked SgK269 overexpression compared with the remainder. Consequently, while SgK269 overexpression does occur in primary basal breast cancers, dysregulation is not restricted to this breast cancer subtype.

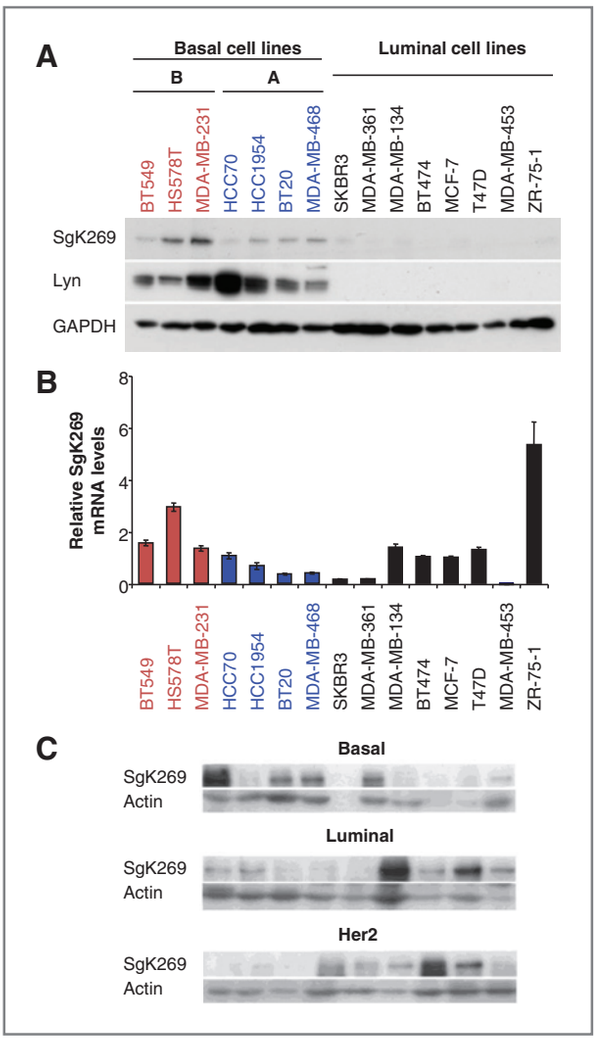

Figure 2. SgK269 protein expression is elevated in basal breast cancer cell lines and a subset of primary breast cancers. A, Western blot analysis of SgK269 and Lyn expression across a panel of breast cancer cell lines. B, SgK269 mRNA expression across breast cancer cell lines. Data are expressed relative to the expression level of MCF-7 cells (mean ± SEM, $n = 3$). C, Western blot analysis of SgK269 expression in different subtypes of primary breast cancer.

SgK269 promotes epithelial-to-mesenchymal transition in mammary epithelial cells

To characterize the functional role of SgK269, we stably expressed SgK269 in MCF-10A immortalized breast epithelial cells at a level approximately 2-fold higher than that in MDA-MB-231 basal breast cancer cells (Fig. 3A). This resulted in cells converting to an elongated, mesenchymal morphology (Fig. 3B) and was associated with a decreased expression of E-cadherin and an increase in N-cadherin (Fig. 3A), indicative of epithelial-to-mesenchymal transition (EMT; ref. 24). To characterize this phenotypic change further, we undertook a comprehensive expression analysis of genes associated with EMT. Of the 63 genes on the array that are normally upregulated during EMT, 12 showed a significant change, and the majority of these (9 of 12) increased in expression. Among the latter class was ZEB2, a known transcriptional repressor of E-cadherin (25). Of the 21 genes normally downregulated, 8 showed a significant change, and the majority (6 of 8) exhibited reduced expression (Fig. 3C). SgK269-overexpressing cells also exhibited a significant increase in random cell motility (Fig. 3D), and fluorescence microscopy revealed that SgK269 localized to cortical actin as well as actin stress fibers and puncta (Fig. 3E and Supplementary Fig. S5).

SgK269 promotes growth of MCF-10A acini in three-dimensional culture

SgK269 overexpression did not alter the proliferation of MCF-10A cells in monolayer culture (Fig. 4A). However, in Matrigel, SgK269-overexpressing cells generated acini approximately twice the diameter of vector controls (Fig. 4B) that

Published OnlineFirst February 1, 2013; DOI: 10.1158/0008-5472.CAN-12-1472

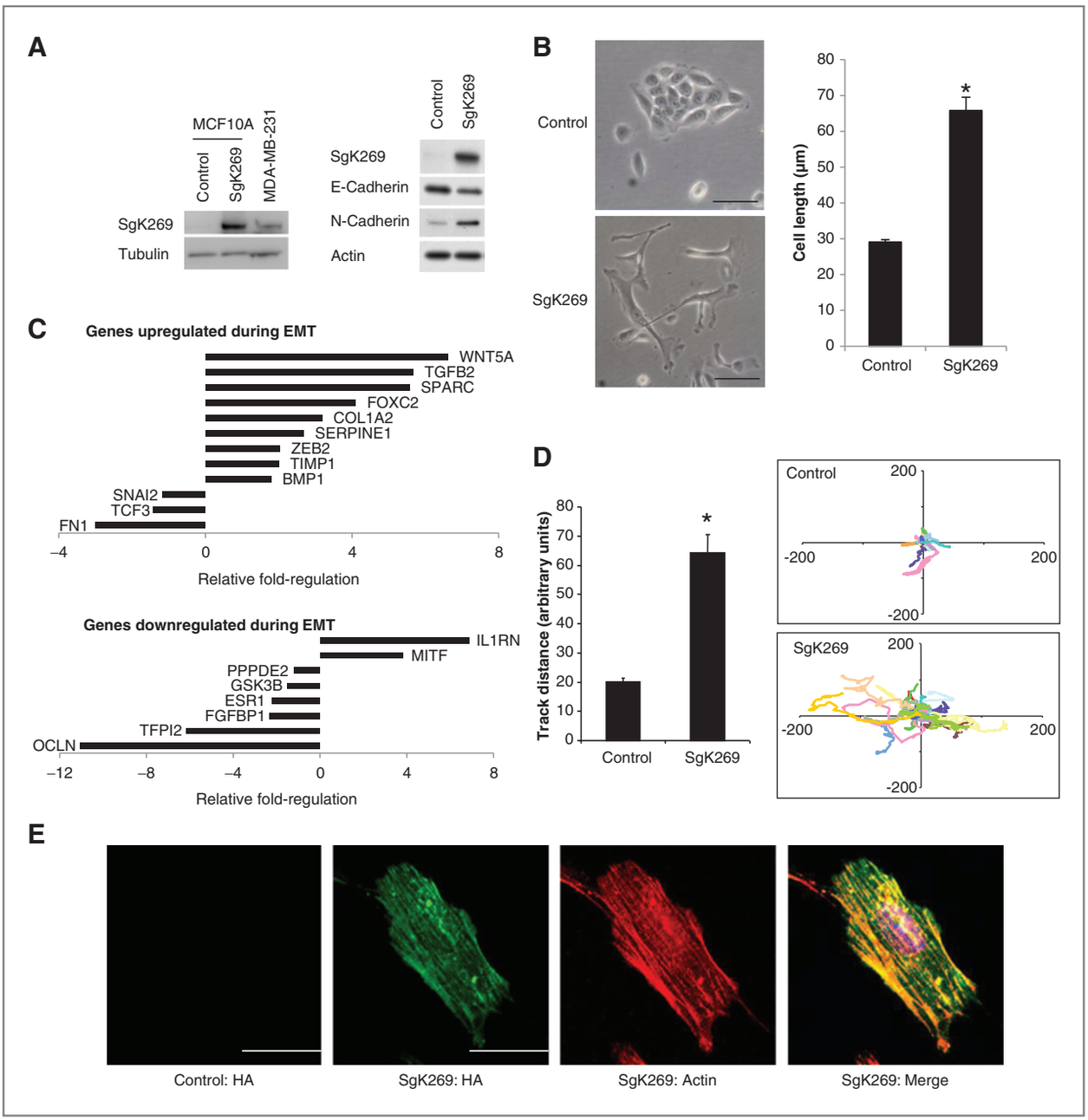

Figure 3. SgK269 promotes EMT in MCF-10A cells. A, SgK269 was stably expressed in MCF-10A cells and cell lysates blotted for the indicated proteins. Left, lysate from MDA-MB-231 basal breast cancer cells was included for comparison. B, photomicrographs of MCF-10A cells expressing SgK269 and vector control cells (scale bar, 50 μm). The histogram on the left indicates mean cell length from the 2 cell populations (mean ± SEM, $n = 100$; *, $P < 0.05$). C, changes in expression of specific EMT markers induced by SgK269. Expression of 84 EMT-related genes was quantified by qRT-PCR and genes exhibiting significant ($P < 0.05$) changes in replicate experiments selected. The graphs indicate fold expression changes in genes normally upregulated (top) or downregulated (bottom) during EMT. D, random cell motility of MCF-10A cells expressing SgK269, as determined by live cell tracking (mean ± SEM, $n = 50$; *, $P < 0.05$). E, fluorescence microscopy of MCF-10A cells expressing SgK269, stained with an anti-HA antibody and phalloidin. Scale bar, 10 μm.

exhibited a distinct, multi-lobular morphology (Fig. 4C) and lacked hollowed lumens (Fig. 4D). In addition, late-stage cultures exhibited prominent Ki67 staining (Fig. 4D), showing that SgK269 signaling overcomes the proliferative suppression that normally occurs following acinar development (26).

Phosphorylation of SgK269 Y635 controls acinar growth and cell invasion

To determine the role of Lyn-mediated SgK269 phosphorylation, we mutated individual Lyn-regulated phosphosites (Y616 and Y635) to phenylalanine and expressed the corresponding mutants in MCF-10A cells (Fig. 5A).

Published OnlineFirst February 1, 2013; DOI: 10.1158/0008-5472.CAN-12-1472

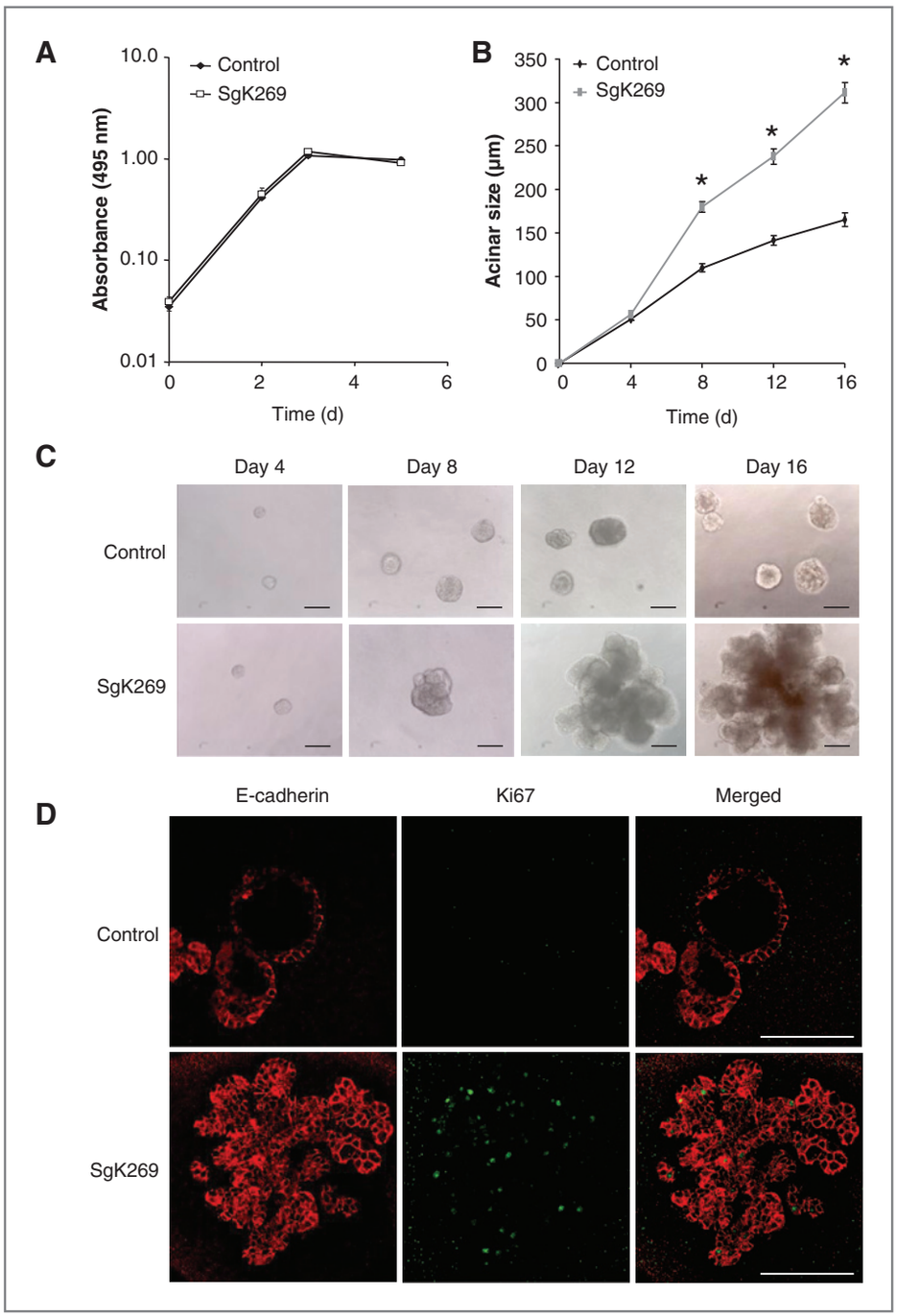

Figure 4. SgK269 promotes growth and abnormal morphology of MCF-10A acini. A, proliferation of vector control and SgK269 expressing MCF-10A cells determined by MTS assay. Data presented are representative of at least 3 independent experiments (mean ± SEM, $n = 6$). B, growth of control and SgK269 expressing MCF-10A acini in Matrigel. Data shown are representative of at least 3 independent experiments (mean ± SEM, $n = 100$; *, $P < 0.05$). C, photomicrographs of MCF-10A acini grown in Matrigel for 12 days. Scale bar, 100 μm. D, fluorescence microscopy of MCF-10A acini grown in Matrigel for 12 days and stained with antibodies against E-cadherin and Ki67. Scale bar, 100 μm.

Anti-phosphotyrosine blotting revealed that neither mutation significantly affected overall SgK269 tyrosine phosphorylation, highlighting the presence of other tyrosine phosphorylation sites (Fig. 5A). Expression of these mutants resulted in a similar elongated cellular morphology to that observed upon overexpression of wild-type (WT) SgK269 (Fig. 5B). Upon three-dimensional (3D) culture, mutation of Y616 was still without effect, but SgK269 Y635F was unable to promote acinar growth to the same degree as WT SgK269 (Fig. 5C and D). SgK269 Y635F–expressing acini still displayed an aberrant, multilobular morphology (Fig. 5C and D), indicating that acinar growth and morphology are regulated by Y635-dependent and -independent pathways, respectively. In Transwell assays, overexpression of SgK269 led to increased cell invasion, but this effect was lost with the Y635F mutant (Fig. 5E).

Phosphorylation-dependent interactions of SgK269

To determine possible interaction partners for the Lyn phosphosites within SgK269, we used NetPhorest (27). On the

Published OnlineFirst February 1, 2013; DOI: 10.1158/0008-5472.CAN-12-1472

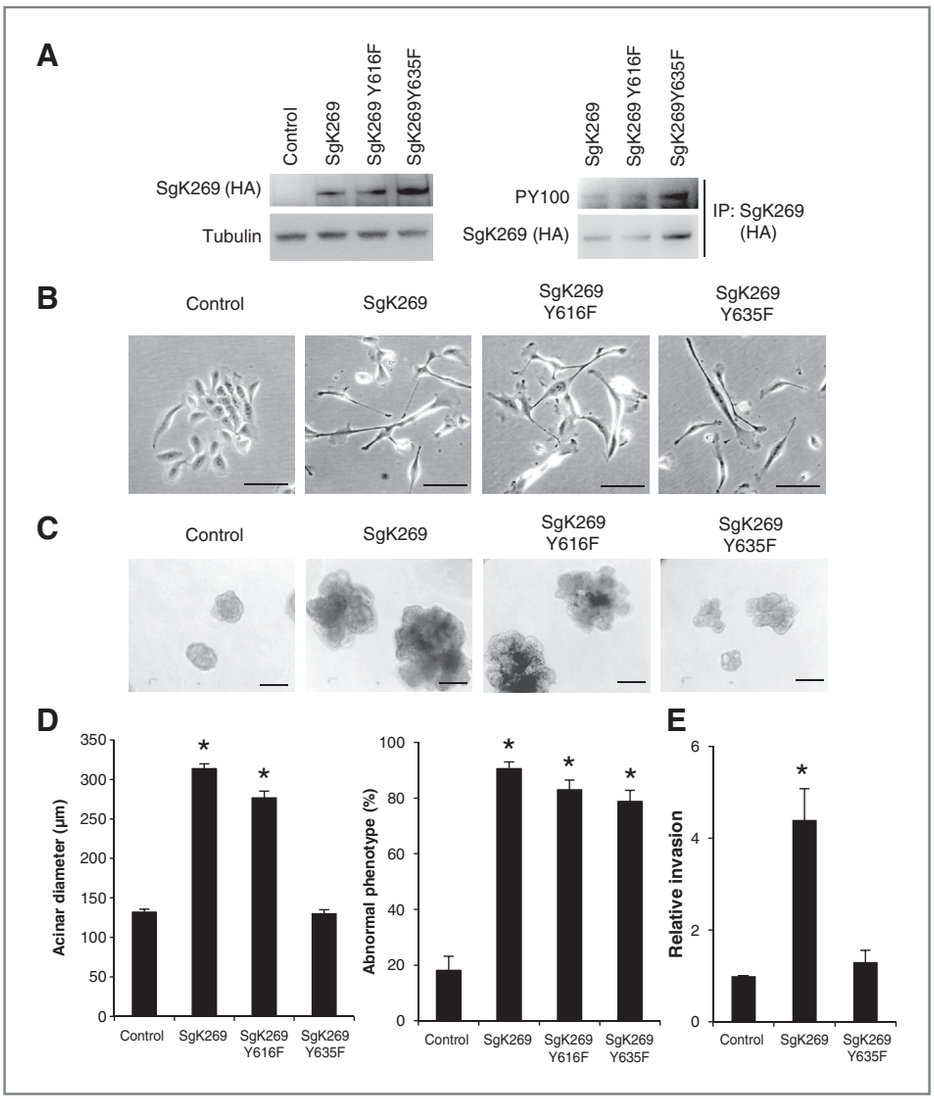

Figure 5. Functional characterization of Lyn phosphosites within SgK269. A, expression and tyrosine phosphorylation of Y616F and Y635F mutants in MCF-10A cells. B, photomicrographs of cells expressing WT and mutant versions of SgK269. Scale bar, 50 μm. C, photomicrographs of acini expressing WT and mutant versions of SgK269. Cells were grown in Matrigel for 12 days. Scale bar, 100 μm. D, left histogram, quantification of acinar diameter following growth in Matrigel for 12 days. Data represent mean ± SEM, $n = 100$. *, $P < 0.01$ relative to vector control acini. Right histogram, quantification of MCF-10A acini presenting abnormal, multilobular morphology. *, $P < 0.01$ relative to vector control acini. E, SgK269 enhances cell invasion in a Y635-dependent manner. Data shown are the mean ± SEM of 3 independent Transwell experiments. *, $P < 0.05$ relative to vector control.

basis of linear amino acid recognition motifs, the most likely binding partner for Y635 was the SH2 domain of Grb2 (posterior probability of 0.51). Immunoprecipitation of WT SgK269 confirmed that it associates with both Shc and Grb2 *in vivo* (Fig. 6A), as well as Crk, which has previously been identified as a SgK269 interactor (3). While the interaction between SgK269 and Shc was not altered for the Y635F mutant, the interaction with Grb2 was decreased by about 50% (Fig. 6B). Given that Y616 and Y1188 both reside within consensus-binding motifs for the Shc PTB domain, it is likely that residual Grb2 binding by the Y635F mutant occurs indirectly via Shc. Consistent with our data identifying the SFK Lyn as a mediator of Y635 phosphorylation (Fig. 1), treatment of basal breast cancer cells with the SFK inhibitor PP2, or Lyn knockdown, led to decreased Y635 phosphorylation and Grb2 association with SgK269 (Fig. 6C and D). Interestingly, Src knockdown did not affect Y635 phosphorylation, indicating a predominant role for Lyn in regulating phosphorylation of this site, but the greatest degree of Src knockdown slightly reduced SgK269/Grb2 association (Supplementary Fig. S6), which may reflect Src-mediated phosphorylation of other sites on SgK269.

In pull-down assays, a GST-Grb2 SH2 fusion protein bound to WT SgK269 but not SgK269 Y635F (Fig. 6E). In addition, binding of SgK269 to this fusion protein was competed by a phosphopeptide corresponding to the Y635 phosphorylation site but not a nonphosphorylated control peptide (Fig. 6E). Overall, these data are consistent with a model where Lyn-mediated phosphorylation of Y635 leads to recruitment of Grb2 via the Grb2 SH2 domain.

Signaling pathway activation downstream of SgK269

For cells grown in monolayer culture, extracellular signal–regulated kinase (Erk) or Akt activation was not altered upon SgK269 overexpression (Fig. 7A). However, phosphorylation of Stat3 at Y705 increased about 3-fold, an effect absent upon expression of SgK269 Y635F. We also conducted Western blotting on acinar lysates from Matrigel cultures.

Published OnlineFirst February 1, 2013; DOI: 10.1158/0008-5472.CAN-12-1472

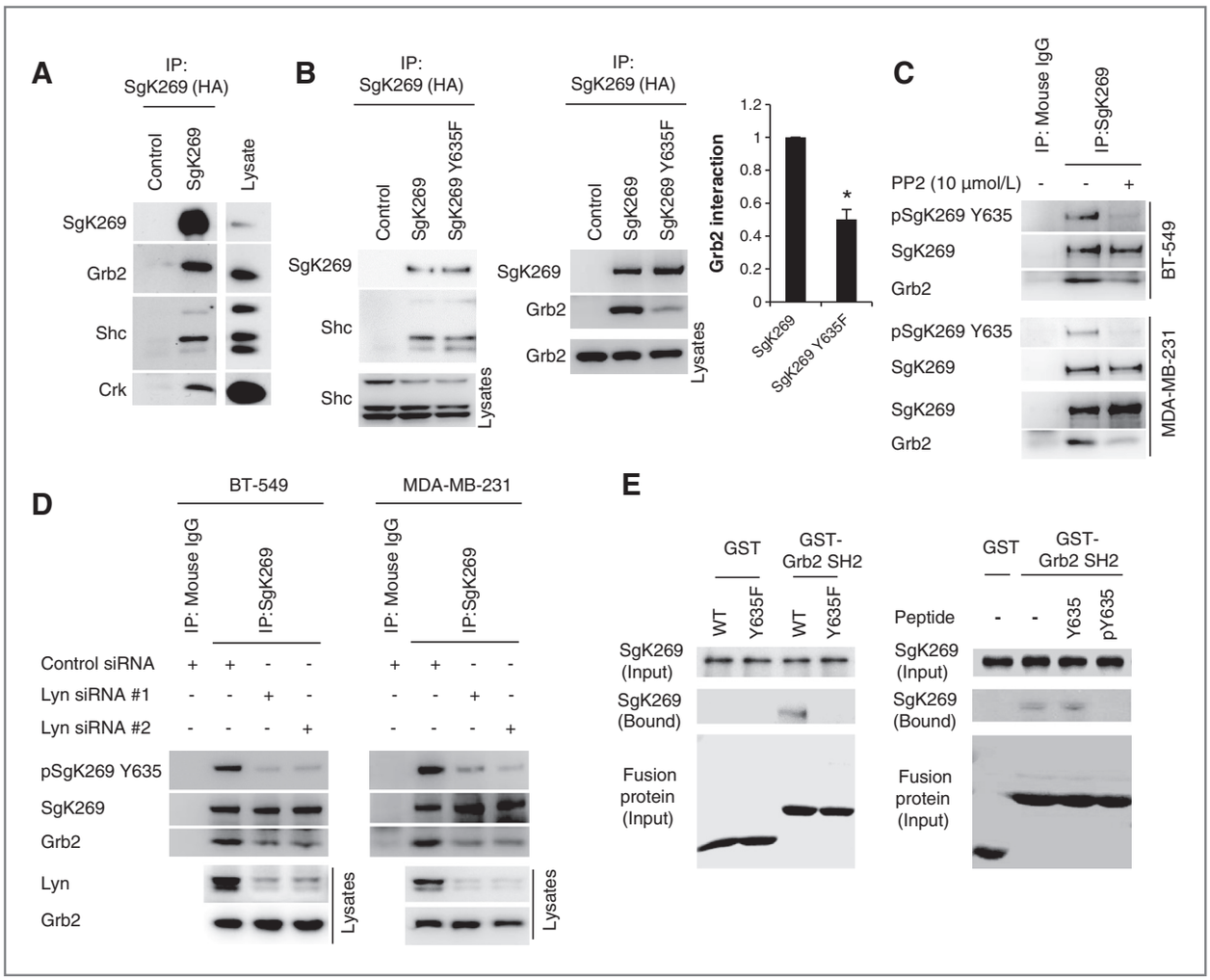

Figure 6. Determination of protein–protein interactions and signaling pathways regulated by Y635 phosphorylation. A, coimmunoprecipitation studies with WT SgK269. B, coimmunoprecipitation of Grb2 and Shc with WT and Y635F SgK269. The histogram provides quantification of the Grb2 interaction with Y635F SgK269 normalized to the respective interaction with WT SgK269. Data represent mean ± SEM, $n = 5$. *, $P < 0.05$. C, effect of the SFK inhibitor PP2 on SgK269/Grb2 interaction. SgK269 immunoprecipitates were Western blotted as indicated. For the experiment from MDA-MB-231 cells, separate immunoprecipitates were Western blotted for pY635 and Grb2, and the loading controls are provided below and above the pY635 and Grb2 blots, respectively. D, effect of Lyn knockdown on SgK269/Grb2 interaction. SgK269 immunoprecipitates and corresponding cell lysates were Western blotted as indicated. E, phosphorylated Y635 represents a binding site for the Grb2 SH2 domain. Left, GST or GST-Grb2 SH2 immobilized on beads was used in pull-down assays from the indicated cell lysates. Bound SgK269 was detected by Western blotting and equal loading confirmed by gel staining with Coomassie Blue. Right, pull-down assays were undertaken in the presence or absence of phosphorylated or nonphosphorylated Y635 peptides.

Under these conditions, SgK269, but not SgK269 Y635F, enhanced phosphorylation of both Erk and Stat3 (Fig. 7A).

To determine the contribution of Erk activation downstream of SgK269 to abnormal growth of MCF-10A acini, cells expressing WT SgK269 were grown in Matrigel in the presence of an MEK inhibitor (PD184352). Low concentrations of MEK inhibitor that were able to negate the increased Erk activation induced upon SgK269 overexpression reduced the size of SgK269-overexpressing acini back to that of vector control acini (Fig. 7B). However, SgK269-overexpressing acini grown in the presence of the MEK inhibitor still exhibited a multilobular phenotype, indicating that MEK/Erk activation downstream of SgK269 Y635 impacts on acinar growth rather than morphogenesis. Because MCF-10A cells were unable to grow in Matrigel in the presence of low concentrations of the Stat3 inhibitor Stattic (data not shown), we could not determine the functional role of SgK269-mediated Stat3 activation.

SgK269 promotes EMT and anchorage-independent growth in basal breast cancer cells

To extend the insights gained from an overexpression model, we manipulated SgK269 expression and signaling in basal breast cancer cell lines. Stable SgK269 knockdown in MDA-MB-231 cells led to acquisition of a more epithelial morphology, increased expression of E-cadherin, and

Published OnlineFirst February 1, 2013; DOI: 10.1158/0008-5472.CAN-12-1472

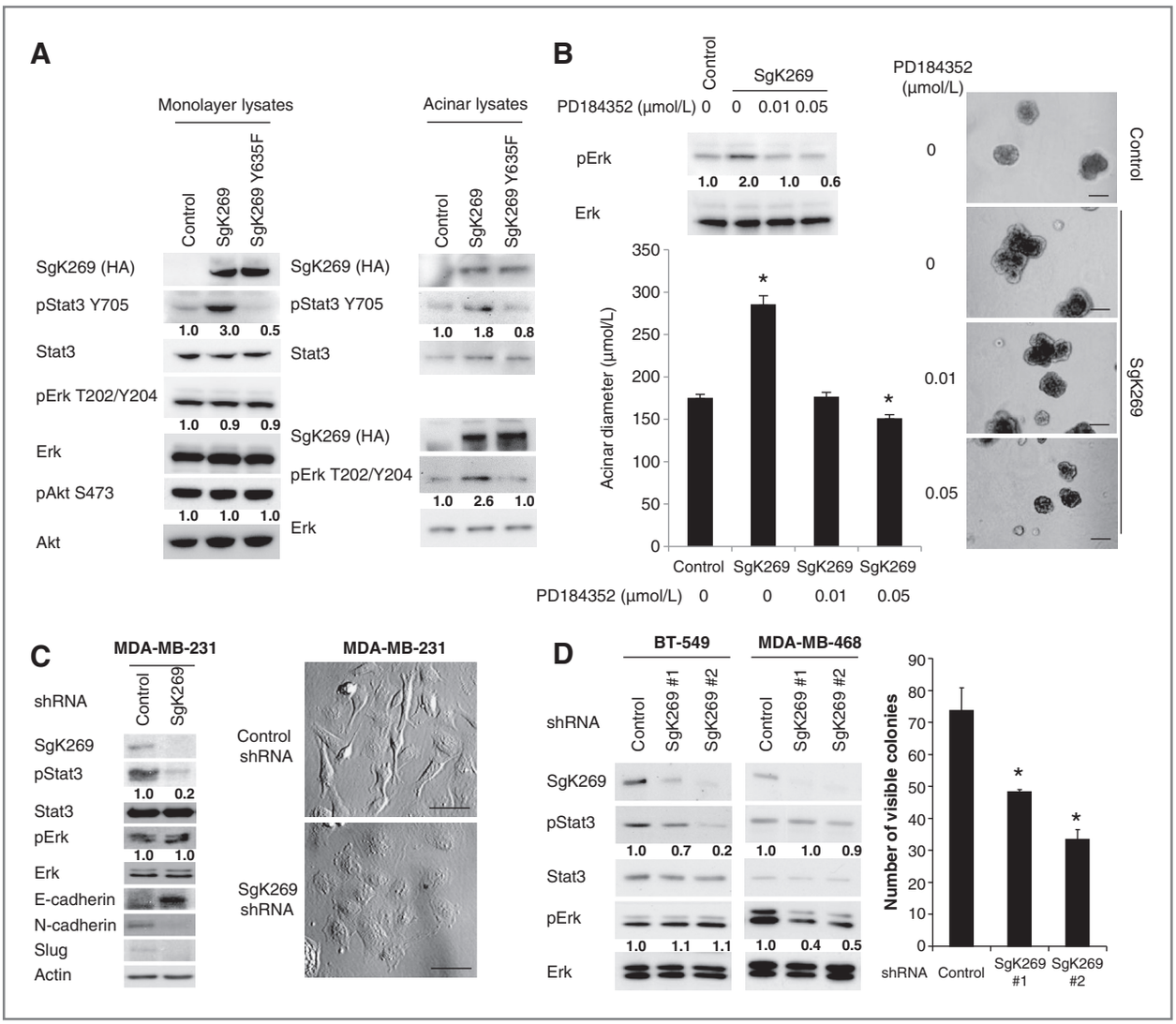

Figure 7. Functional analysis of SgK269 in MCF-10A and basal breast cancer cells. A, signaling pathway activation in MCF-10A cells. Cell lysates from monolayers or 3D cultures grown for 4 days were Western blotted as indicated. Numbers below the panels indicate normalized (relative to total) levels of pStat3, pErk, and pAkt, expressed relative to the value for vector controls, which is arbitrarily set at 1.0. B, MEK inhibition reverses the effect of SgK269 on acinar size. Top left, Western blotting on acinar lysates grown for 4 days in the presence of PD184352 at the indicated concentrations. Right, photomicrographs and bottom left, acinar size quantification, of the corresponding acini grown in Matrigel for 12 days. Data represent mean ± SEM, $n = 100$. *, $P < 0.05$ relative to vector control acini. Scale bar, 100 μm. C, stable SgK269 knockdown in MDA-MB-231 cells induces mesenchymal-to-epithelial transition. Left, lysates from control and SgK269 knockdown cells were Western blotted as indicated. Right, morphology of the corresponding cell pools, as indicated by light microscopy. Scale bar, 50 μm. D, effect of stable SgK269 knockdown in BT-549 and MDA-MB-468 basal breast cancer cells. Cell lysates were Western blotted with the indicated antibodies. The histogram provides the results for anchorage-independent growth assays where control or SgK269 knockdown BT549 cells were grown in soft agar for 14 days. Data represent mean ± SEM, $n = 3$. *, $P < 0.05$.

reduced levels of both N-cadherin and Slug, consistent with mesenchymal-to-epithelial transition. While Erk activation was unchanged, Stat3 activation was markedly reduced (Fig. 7C). The knockdown cells also exhibited decreased viability at low serum concentrations (Supplementary Fig. S7A). When WT SgK269 was overexpressed in MDA-MB-231 cells, which exhibit relatively high endogenous levels of this protein, a trend for enhanced anchorage-independent growth relative to controls was observed. However, expression of SgK269 Y635F significantly reduced colony formation, indicating a dominant-negative effect of the mutant (Supplementary Fig. S7B and S7C). SgK269 knockdown in BT-549 cells resulted in decreased Stat3 activation, whereas there was no change in Erk activity (Fig. 7D). However, SgK269 knockdown in MDA-MB-468 cells did not alter Stat3 activity, but Erk activity was decreased (Fig. 7D). These findings confirm that endogenous SgK269 can modulate Stat3 and Erk signaling but indicate that the effect on either

Published OnlineFirst February 1, 2013; DOI: 10.1158/0008-5472.CAN-12-1472

pathway can be context-dependent. Importantly, the knockdown of SgK269 in BT-549 cells reduced their ability to grow under anchorage-independent conditions (Fig. 7D).

Discussion

Recently, we determined that basal breast cancer cells are characterized by a prominent SFK signaling network that features high expression of the SFK Lyn. In the manuscript, we show that Lyn positively regulates the phosphorylation of a small subset of proteins within this network that includes the atypical kinase SgK269. In addition, we identify novel Lyn-regulated signaling roles for SgK269.

Lyn has been extensively characterized in the hematopoietic system (28, 29), although it also has an emerging role in solid malignancies (2, 30, 31). This study represents the first detailed phosphoproteomic analysis of Lyn substrates in the latter context. Within the hematopoietic compartment Lyn can have both positive and negative regulatory roles in signal propagation and known Lyn substrates include inhibitory receptors (PIR-B and SIRP-α) and phosphatases (SHP-1 and SHIP-1), the DOK-1 and Gab2 docking proteins, and the adaptor CrkL (28, 29). CrkL represents the only overlap between proteins identified by our screen and these hematopoietic substrates, presumably reflecting the contrasting expression profile of particular Lyn targets in hematopoietic versus epithelial cells as well as that of receptors/scaffolds that regulate access of Lyn to particular substrates. However, a consistent feature of Lyn substrates in both cell types is that they often represent transmembrane proteins or components of plasma membrane–localized signaling complexes. Many of our identified targets are not documented as known substrates of Lyn or other SFKs. These include ribosomal subunit 10, ADAM9, TGFR1, and OSMR.

The Klemke group reported a weak *in vitro* tyrosine kinase activity for SgK269 (3), and in recently published work, showed a proproliferative role for this activity (12). However, our study is the first to show that Lyn-mediated phosphorylation of Y635 imparts a potent scaffolding function to this protein. Phosphorylation of Y635 was required for SgK269 to promote activation of Erk and Stat3 in 3D culture, cell invasion, and acinar growth, and careful titration of a selective MEK inhibitor confirmed the contribution of the MEK/Erk pathway to the latter biologic response. Stimulation of Erk activation by SgK269 is consistent with Y635-mediated recruitment of Grb2 leading to Sos-mediated Ras activation, which could occur at cellular sites where SgK269 is in close proximity to the plasma membrane, for example, at the cell cortex or focal adhesions (3). However, how Y635 phosphorylation leads to Stat3 activation is unclear at present. Because we have been unable to coimmunoprecipitate SgK269 with Stat3 (Croucher and Daly, unpublished data), SgK269 does not appear to act as a scaffold for Stat3 and the corresponding kinase, but it remains possible that phosphorylated Y635 activates such a kinase either directly or via Grb2. A candidate intermediary is Syk because phosphorylated Y635 is predicted to bind the Syk SH2 domains (27, 32). An alternative model involves Y635-dependent sequestration of Grb2 by SgK269 leading to enhanced recruitment and phosphorylation of Stat3 by the EGFR, which could occur because Grb2 and Stat3 compete for the same binding sites on this receptor (33).

Aside from promotion of acinar growth, the other major effect induced by SgK269 in MCF-10As was acquisition of an elongated and highly motile phenotype and perturbed acinar morphogenesis. Interestingly, these effects do not appear to be driven by effects of SgK269 on Erk or Stat3 signaling, as Erk activation was not affected by SgK269 in monolayer culture, inhibition of MEK/Erk signaling attenuated growth, but not aberrant morphogenesis, of SgK269-overexpressing acini, and SgK269 Y635F, which does not promote Stat3 or Erk activation, still altered cell morphology in monolayer and 3D culture. In addition, SgK269-induced morphologic effects were independent of Y616 phosphorylation. The most likely explanation for these effects is that SgK269 perturbs cytoskeletal organization, either by directly phosphorylating regulators of the actin cytoskeleton, and/or by its scaffolding function. Consistent with this hypothesis, SgK269 associates with Crk and BCAR1/p130Cas (3), known regulators of Rac and Rap GTPases and hence cell spreading and migration (34). Furthermore, in addition to Y616 and Y635, SgK269 contains further known and predicted sites of tyrosine phosphorylation, including Y387, Y641, and Y1188 (2, 3), that could recruit SH2 or PTB domain–containing effectors. Either the direct (kinase-dependent) or indirect (scaffolding) signaling mechanism would be facilitated by localization of SgK269 to the actin cytoskeleton. Overall, our data highlight the capacity of SgK269 to generate several different signal outputs and thereby modulate both cell proliferation and migration.

Importantly, our functional characterization of SgK269 in basal breast cancer cells supports the pathophysiologic relevance of data from the MCF-10A model. This showed that SgK269 is required for maintenance of a mesenchymal phenotype in MDA-MB-231 cells and promotes Stat3 or Erk activation, depending on the cell line. In addition, SgK269 enhanced anchorage-independent growth, a key characteristic of the transformed phenotype, and this activity was dependent on Y635 phosphorylation. Finally, our finding that the invasive potential of SgK269-overexpressing MCF-10A cells, which express high levels of Lyn (our unpublished data), is dependent on Y635 phosphorylation is consistent with our previous observation that Lyn knockdown markedly reduces invasion of basal breast cancer cells (2).

Our characterization of the network roles of Lyn and SgK269 highlights potential strategies for improved treatment of basal breast cancers, as well as other breast cancer subtypes where SgK269 is overexpressed. SgK269 kinase activity may represent a target for therapeutic intervention with small-molecule kinase inhibitors, and if SgK269 activates Stat3 via an indirect mechanism, then Stat3 kinases that act downstream of SgK269 may also represent therapeutic targets. Finally, given its signaling role downstream of multiple tyrosine kinases (6–11), and recent data showing that SgK269 modulates cellular sensitivity to trastuzumab (12), it will be interesting to determine whether SgK269

represents a biomarker of therapeutic responsiveness that could be used for improved patient stratification for targeted therapy.

Disclosure of Potential Conflicts of Interest

No potential conflicts of interest were disclosed.

Authors' Contributions

Conception and design: D.R. Croucher, F. Hochgräfe, R.J. Daly
Development of methodology: D.R. Croucher, F. Hochgräfe, R.J. Lyons, C.M. Tactacan, R. Shearer, D.N. Saunders
Acquisition of data (provided animals, acquired and managed patients, provided facilities, etc.): D.R. Croucher, F. Hochgräfe, L. Zhang, L. Liu, C.M. Tactacan, B.C. Browne, N. Ali, R. Shearer, D.N. Saunders, A. Swarbrick
Analysis and interpretation of data (e.g., statistical analysis, biostatistics, computational analysis): D.R. Croucher, F. Hochgräfe, L. Liu, C.M. Tactacan, N. Ali, H. Chan, D.N. Saunders, R.J. Daly
Writing, review, and/or revision of the manuscript: D.R. Croucher, R.J. Lyons, N. Ali, R.J. Daly
Administrative, technical, or material support (i.e., reporting or organizing data, constructing databases): D. Rickwood, D. Gallego-Ortega
Study supervision: A. Swarbrick, R.J. Daly

Grant Support

This work was supported by research grants from the National Health and Medical Research Council of Australia, Cancer Council New South Wales (NSW) and Science Foundation Ireland (Grant No. 06/CE/B1129). D.R. Croucher and D. N. Saunders were supported by Fellowships from Cancer Institute (CI) NSW. F. Hochgräfe is supported by The Ministry of Education and Research, Bundesministerium für Bildung und Forschung (03Z1CN21). C.M. Tactacan is the recipient of a Research Scholarship from CINSW and L. Zhang is an Australian Postgraduate Award recipient. DGO is supported by a National Breast Cancer Foundation (NBCF) and Cure Cancer Australia Foundation Postdoctoral Fellowship. A. Swarbrick is supported by an Early Career Fellowship from the NBCF.

The costs of publication of this article were defrayed in part by the payment of page charges. This article must therefore be hereby marked *advertisement* in accordance with 18 U.S.C. Section 1734 solely to indicate this fact.

Received April 23, 2012; revised November 5, 2012; accepted November 23, 2012; published OnlineFirst February 1, 2013.

References

1. Rakha EA, Reis-Filho JS, Ellis IO. Basal-like breast cancer: a critical review. J Clin Oncol 2008;26:2568–81.
2. Hochgrafe F, Zhang L, O'Toole SA, Browne BC, Pinese M, Porta Cubas A, et al. Tyrosine phosphorylation profiling reveals the signaling network characteristics of Basal breast cancer cells. Cancer Res 2010; 70:9391–401.
3. Wang Y, Kelber JA, Tran Cao HS, Cantin GT, Lin R, Wang W, et al. Pseudopodium-enriched atypical kinase 1 regulates the cytoskeleton and cancer progression [corrected]. Proc Natl Acad Sci U S A 2010;107:10920–5.
4. Manning G, Whyte DB, Martinez R, Hunter T, Sudarsanam S. The protein kinase complement of the human genome. Science (New York, NY) 2002;298:1912–34.
5. Boudeau J, Miranda-Saavedra D, Barton GJ, Alessi DR. Emerging roles of pseudokinases. Trends Cell Biol 2006;16:443–52.
6. Leroy C, Fialin C, Sirvent A, Simon V, Urbach S, Poncet J, et al. Quantitative phosphoproteomics reveals a cluster of tyrosine kinases that mediates SRC invasive activity in advanced colon carcinoma cells. Cancer Res 2009;69:2279–86.
7. Luo W, Slebos RJ, Hill S, Li M, Brábek J, Amanchy R, et al. Global impact of oncogenic Src on a phosphotyrosine proteome. J Proteome Res 2008;7:3447–60.
8. Bonnette PC, Robinson BS, Silva JC, Stokes MP, Brosius AD, Baumann A, et al. Phosphoproteomic characterization of PYK2 signaling pathways involved in osteogenesis. J Proteomics 2010;73:1306–20.
9. Boersema PJ, Foong LY, Ding VM, Lemeer S, van Breukelen B, Philp R, et al. In-depth qualitative and quantitative profiling of tyrosine phosphorylation using a combination of phosphopeptide immunoaffinity purification and stable isotope dimethyl labeling. Mol Cell Proteomics 2010;9:84–99.
10. Zhang G, Fenyo D, Neubert TA. Screening for EphB signaling effectors using SILAC with a linear ion trap-orbitrap mass spectrometer. J Proteome Res 2008;7:4715–26.
11. Guo A, Villen J, Kornhauser J, Lee KA, Stokes MP, Rikova K, et al. Signaling networks assembled by oncogenic EGFR and c-Met. Proc Natl Acad Sci U S A 2008;105:692–7.
12. Kelber JA, Reno T, Kaushal S, Metildi C, Wright T, Stoletov K, et al. KRas induces a Src/PEAK1/ErbB2 kinase amplification loop that drives metastatic growth and therapy resistance in pancreatic cancer. Cancer Res 2012;72:2554–64.
13. Croucher DR, Rickwood D, Tactacan CM, Musgrove EA, Daly RJ. Cortactin modulates RhoA activation and expression of Cip/Kip cyclin-dependent kinase inhibitors to promote cell cycle progression in 11q13-amplified head and neck squamous cell carcinoma cells. Mol Cell Biol 2010;30:5057–70.
14. Brummer T, Schramek D, Hayes VM, Bennett HL, Caldon CE, Musgrove EA, et al. Increased proliferation and altered growth factor dependence of human mammary epithelial cells overexpressing the Gab2 docking protein. J Biol Chem 2006;281:626–37.
15. deFazio A, Chiew YE, Sini RL, Janes PW, Sutherland RL. Expression of c-erbB receptors, heregulin and oestrogen receptor in human breast cell lines. Int J Cancer 2000;87:487–98.
16. Herrera Abreu MT, Hughes WE, Mele K, Lyons RJ, Rickwood D, Browne BC, et al. Gab2 regulates cytoskeletal organization and migration of mammary epithelial cells by modulating RhoA activation. Mol Biol Cell 2011;22:105–16.
17. Ong SE, Blagoev B, Kratchmarova I, Kristensen DB, Steen H, Pandey A, et al. Stable isotope labeling by amino acids in cell culture, SILAC, as a simple and accurate approach to expression proteomics. Mol Cell Proteomics 2002;1:376–86.
18. Rush J, Moritz A, Lee KA, Guo A, Goss VL, Spek EJ, et al. Immunoaffinity profiling of tyrosine phosphorylation in cancer cells. Nat Biotechnol 2005;23:94–101.
19. Pan C, Kumar C, Bohl S, Klingmueller U, Mann M. Comparative proteomic phenotyping of cell lines and primary cells to assess preservation of cell type-specific functions. Mol Cell Proteomics 2009;8:443–50.
20. Lowenstein EJ, Daly RJ, Batzer AG, Li W, Margolis B, Lammers R, et al. The SH2 and SH3 domain-containing protein GRB2 links receptor tyrosine kinases to ras signaling. Cell 1992;70:431–42.
21. Janes PW, Lackmann M, Church WB, Sanderson GM, Sutherland RL, Daly RJ. Structural determinants of the interaction between the erbB2 receptor and the Src homology 2 domain of Grb7. J Biol Chem 1997;272:8490–7.
22. Croucher DR, Saunders DN, Stillfried GE, Ranson M. A structural basis for differential cell signalling by PAI-1 and PAI-2 in breast cancer cells. Biochem J 2007;408:203–10.
23. Matsuda D, Nakayama Y, Horimoto S, Kuga T, Ikeda K, Kasahara K, et al. Involvement of Golgi-associated Lyn tyrosine kinase in the translocation of annexin II to the endoplasmic reticulum under oxidative stress. Exp Cell Res 2006;312:1205–17.
24. Gravdal K, Halvorsen OJ, Haukaas SA, Akslen LA. A switch from E-cadherin to N-cadherin expression indicates epithelial to mesenchymal transition and is of strong and independent importance for the progress of prostate cancer. Clin Cancer Res 2007;13:7003–11.
25. Peinado H, Olmeda D, Cano A. Snail, Zeb and bHLH factors in tumour progression: an alliance against the epithelial phenotype? Nat Rev Cancer 2007;7:415–28.
26. Debnath J, Muthuswamy SK, Brugge JS. Morphogenesis and oncogenesis of MCF-10A mammary epithelial acini grown in three-dimensional basement membrane cultures. Methods 2003;30:256–68.
27. Miller ML, Jensen LJ, Diella F, Jørgensen C, Tinti M, Li L, et al. Linear motif atlas for phosphorylation-dependent signaling. Sci Signal 2008;1:ra2.

Published OnlineFirst February 1, 2013; DOI: 10.1158/0008-5472.CAN-12-1472

28. Hibbs ML, Harder KW. The duplicitous nature of the Lyn tyrosine kinase in growth factor signaling. Growth Factors 2006;24:137–49.
29. Scapini P, Pereira S, Zhang H, Lowell CA. Multiple roles of Lyn kinase in myeloid cell signaling and function. Immunol Rev 2009;228:23–40.
30. Choi YL, Bocanegra M, Kwon MJ, Shin YK, Nam SJ, Yang JH, et al. LYN is a mediator of epithelial-mesenchymal transition and a target of dasatinib in breast cancer. Cancer Res 2010;70:2296–306.
31. Park SI, Zhang J, Phillips KA, Araujo JC, Najjar AM, Volgin AY, et al. Targeting SRC family kinases inhibits growth and lymph node metastases of prostate cancer in an orthotopic nude mouse model. Cancer Res 2008;68:3323–33.
32. Uckun FM, Qazi S, Ma H, Tuel-Ahlgren L, Ozer Z. STAT3 is a substrate of SYK tyrosine kinase in B-lineage leukemia/lymphoma cells exposed to oxidative stress. Proc Natl Acad Sci U S A 2010;107:2902–7.
33. Zhang T, Ma J, Cao X. Grb2 regulates Stat3 activation negatively in epidermal growth factor signalling. Biochem J 2003;376:457–64.
34. Defilippi P, Di Stefano P, Cabodi S. p130Cas: a versatile scaffold in signaling networks. Trends Cell Biol 2006;16:257–63.